PAPER • OPEN ACCESS

Exploring fusion-reactor physics with high-power electron cyclotron resonance heating on ASDEX Upgrade

View the article online for updates and enhancements.

Exploring fusion-reactor physics with high-power electron cyclotron resonance heating on ASDEX Upgrade

**J Stober[1] , M Reisner[1], C Angioni[1], A Bañón Navarro[1] , V Bobkov[1],
A Bock[1], G Denisov[2], E Fable[1], R Fischer[1], G Gantenbein[6], L Gil[3],
T Görler[1] , V Igochine[1] , W Kasparek[4], F Leuterer[1], A Litvak[2],
R McDermott[1] , A Meier[5], F Monaco[1], M Münich[1], V Nichiporenko[7],
B Plaum[4], U Plank[1], E Poli[1], L Popov[7], Th Pütterich[1] , Th Scherer[5],
M Schubert[1], W Suttrop[1], E Tai[7], M Thumm[6], D Wagner[1], H Zohm[1], MST1
team[8] and the ASDEX Upgrade team[1]**

[1] Max-Planck-Institut für Plasmaphysik, Garching, Germany
[2] Institute of Applied Physics, Nizhny Novgorod, Russia
[3] IPFN, Instituto Superior Técnico, Universidade Lisboa, Portugal
[4] IGVP, Universität Stuttgart, Germany
[5] IAM, Karlsruhe Institute for Technology, Germany
[6] IHM, Karlsruhe Institute for Technology, Germany
[7] GYCOM Ltd, Nizhny Novgorod and Moscow, Russia

E-mail: Joerg.Stober@ipp.mpg.de

CrossMark

Abstract

The electron cyclotron resonance heating (ECRH) system of the ASDEX Upgrade tokomak has been upgraded over the last 15 years from a 2 MW, 2 s, 140 GHz system to an 8 MW, 10 s, dual frequency system (105/140 GHz). The power exceeds the L/H power threshold by at least a factor of two, even for high densities, and roughly equals the installed ion cyclotron range of frequencies power. The power of both wave heating systems together (>10 MW in the plasma) is about half of the available neutral beam injection (NBI) power, allowing significant variations of torque input, of the shape of the heating profile and of Qe/Qi, even at high heating power. For applications at a low magnetic field an X3-heating scheme is routinely in use. Such a scenario is now also forseen for ITER to study the first H-modes at one third of the full field. This versatile system allows one to address important issues fundamental to a fusion reactor: H-mode operation with dominant electron heating, accessing low collisionalities in full metal devices (also related to suppression of edge localized modes with resonant magnetic perturbations), influence of Te/Ti and rotational shear on transport, and dependence of impurity accumulation on heating profiles. Experiments on all these subjects have been carried out over the last few years and will be presented in this contribution. The adjustable localized current drive capability of ECRH allows dedicated variations of the shape of the q-profile and the study of their influence on non-inductive tokamak operation (so far at $q_{95} > 5.3$). The ultimate goal of these experiments is to use the experimental findings to

[8] Ses: B. Labit et al, 2019 Nucl. Fusion 59 086020.

refine theoretical models such that they allow a reliable design of operational schemes for reactor size devices. In this respect, recent studies comparing a quasi-linear approach (TGLF) with fully non-linear modeling (GENE) of non-inductive high-beta plasmas will be reported.

Keywords: Tokamak, ECRH, ECCD, q-profile, non-inductive, high-beta

(Some figures may appear in colour only in the online journal)

1. Introduction

The invited EPS talk, to which this paper is assigned, mostly had the characteristics of an overview of the electron cyclotron resonance heating (ECRH) results from the ASDEX Upgrade (AUG). Therefore, the main purpose of the paper is to summarize the presented material together with a short historical review and an extensive list of references, in this case strongly biased towards AUG. Additionally, some points of relevance, especially for ITER and beyond, are described and discussed in more detail.

A key point of the paper is to illustrate the interplay between the technical possibilities of mm-wave heating on one side and the demands from the experiment on the other side, which themselves continue to develop as the heating system is routinely, reliably and successfully applied in the experiments. To give the paper a readable structure this interplay has to be disentangled: section 2 starts describing the evolution of the EC system of AUG using forward references to the studies of fusion-reactor physics described in section 3 and vice versa. In the last subsection of section 3 the interpretation of high β experiments aiming at non-inductive operation of a reactor will be compared for quasi-linear and fully non-linear gyrokinetic modeling, especially with the relevance to ExB flow shearing. The paper closes with a general discussion that also includes the consequences of the findings presented here on control of burning fusion plasmas using EC.

This introduction closes with some basics on the EC application used in all sections. For more details see [1]. Here, we only treat the case of waves propagating on one of the two branches of the dispersion relation which include vacuum propagation as the zero density limit, such that the antennas can be located safely far away from the plasma on the low-field side, in contrary to wave-heating applications using lower frequencies. The branches are orthogonally polarized, called O-mode and (fast) X-mode. Free-space wavelengths on AUG are $\lambda \approx 2$–3 mm. EC radiation is transported as beams with cross sections of $d \approx 10$–$100 \times \lambda$ either purely quasi-optically (using refocusing mirrors) or using highly oversized waveguides. Typically, launchers (antennas) are quasi-optical sections, focusing the beam close to the plasma center with the last mirror able to rotate around two axes allowing poloidal and toroidal steering of the beam. Two flat mirrors in the beam line are typically grooved and may be rotated around their surface normals to set any polarization state, which has to match the desired polarization (X or O) at the plasma edge. It is, in general, elliptical and depends on the angle between $\vec{k}$ and $\vec{B}$. Absorption is significant at $\omega \approx n\omega_{ce}$

with n $=$ 2, 3 for X-mode and n $=$ 1, 2 for O-mode. The highest optical depth has X2 followed by O1, X3 and O2. The choice of the heating scheme depends on the available frequencies, the desired magnetic field and potential cutoffs (ω_{pe}, ω_{RH}) for O- and X-mode. These density limitations depend on the size and aspect ratio of a tokamak. They do limit O1 and very high density X2 operation on AUG, but will not hamper operation at ITER at all, since the crucial quantity B^2/n_e is much larger in ITER. Indeed, ITER can use its 170 GHz systems with O1 at full magnetic field, X2 at half field and X3 at one third field. For perpendicular launch in AUG the optical thickness of central X2 heating exceeds 100 by far, and the beam is fully absorbed within a few mm close to the resonance. Given a beam diameter of ≈ 3 cm in AUG, the power of 1 MW is deposited within less than 10 cm^3. If that volume was filled with water it would be evaporated within less than 30 ms. Still, for machines of the size of AUG and bigger, non-linear effects play hardly any role, and beam absorption is well described by linear theory. Beam propagation and absorption are typically handled by ray- or beam-tracing models, taking into account refraction by gradients in the refractive index N and (de)focusing. These models also handle EC current drive (ECCD), which occurs for a toroidally inclined launch. Variations in the poloidal angle are typically used to vary the absorption location across flux surfaces. Work on AUG generally relies on TORBEAM [2] as the beam-tracing code. EC waves interact in the linear regime only with electrons and deliver pure electron heating.

2. Evolution of the EC system and EC heating schemes for AUG

ECRH on AUG started in 1992 with the construction of a 140 GHz system with four beam lines based on GYCOM gyrotrons in collaboration with IAP Nizhny Novgorod, IPF Uni Stuttgart and KIT Karlsruhe. Each gyrotron was capable of operating either 2 s at 0.5 MW or 1 s at 0.7 MW with about 20% loss in transmission. Details can be found in [3] and the references therein. Highlights in plasma research were studies of non-linearities of heat transport using heat-pulse analysis [4, 5], effects of the EC on density peaking depending on collisionality [6], stabilization of neoclassical tearing modes (NTM) [7, 8] and sawtooth (de)stabilization with ECCD [9–11]. The system was operated only with the X2-scheme, and the frequency was chosen for central heating at $B_t = 2.5$ T corresponding to q$_{95}$ > 3.5, having in mind also off-axis ECCD applications at the high-field side at lower B_t. Driven by the successful proof-of-principle experiments on

NTM stabilization a new EC system was planned [12] with the key requirements of sufficient power (4 × 1 MW) and pulse length (10 s) and launcher-mirror movements on time scales well below an energy confinement time in order to establish real-time NTM control. To make the system more versatile with respect to the choice of B_t, multi-frequency gyrotrons and a broadband transmission line were pioneered by the same partnership as for the first system. The first long-pulse high-power two-frequency gyrotron (105/140 GHz) was operated on AUG in 2006 [13], but only in 2014 was the system completed as a 2f-system [14]. Major difficulties were the windows for step-tunable operation (beyond the single-disk Fabry–Perot effect, unresolved so far), and issues related to body-voltage insulation, cryo-magnets or cathode coating, which were solved and taken into account for the design of the Russian ITER gyrotrons. Despite the infancy problems of the system, gyrotron operation at two distinct frequencies fulfilling the Fabry–Perot condition $d = n\frac{\lambda}{2}$ (d: thickness of window disk) has proven to be very robust from the very beginning. Its full potential was demonstrated for the Japanese ITER gyrotron using a triode gun [15]. This option was originally not included in the ITER EC but is now one of the options for operation of ITER at one third of the full magnetic field [16]. Real-time NTM control of (3, 2) and (2, 1) NTMs was demonstrated in 2014 [17]. This control and its further evolution is not part of this paper.

Regular plasma operation with the first gyrotron of the new system started when all plasma facing components of AUG were fully tungsten(W)-coated (2007). As discussed in section 3.1, centrally deposited EC turned out to help prevent W accumulation. In this context X3 and O2 schemes were implemented to either allow operation at a lower magnetic field (similar to the low-field ITER case) or at densities above the X-mode cutoff. Both scenarios were developed for regular use [18] supported by the protective sniffer-probe arrays and additional machine hardening [19]. Extensive operational experience is available in these applications with incomplete single pass absorption, including the use of refocusing holographic reflectors for effective use of the power not absorbed in the first pass [20, 21].

Driven by the need to avoid W accumulation, the EC was recognized by the team as a basic system necessary for operation rather than being a tool for specialists. In 2010 further upgrading of the EC system for AUG was discussed. As an additional physics application, high-power EC was envisaged as a tool to study advanced tokamak physics, i.e. especially for studying the plasma performance for non-standard current profiles, as discussed in section 3.3. The layout of this second upgrade was close to that of the first upgrade also aiming for similar performance (4 × 1 MW, 2 freq.). Major technical innovations were the use of cryogen-free magnets and newly-developed semi-conductor-based body-voltage modulators together with FuG, Rosenheim, Germany. For the main (cathode) power supplies, equipment from the dismantled HERA storage ring from DESY could be reused, requiring the usage of tetrode-based fast high-precision series-modulators. The decision to finance the system

was taken in 2012. The worldwide call for tender for the gyrotrons with all magnets was won by GYCOM Ltd with JASTEC Inc., Japan as a subcontractor for the super-conducting magnets. Plasma experiments with two new beam lines started in 2017, and two more followed in 2018. The system uses the launching positions of the original EC system from 1992, which was dismantled by the end of 2015. The launcher optics had to be modified to replace the large boron-nitride windows with smaller diamond windows. To allow real-time control of the launcher movements within the time scale of current diffusion, the gearings have been revisited and rebuilt together with gearing experts (FZG, TU Munich). Planning with movements not faster than that time scale allowed the system to stay with the small size and position of the rotary feed-throughs, which limit the torque but allow a modular transition from the old to the new gearings. For movements within the time scale of the energy confinement time, as is necessary for NTM stabilization, the four dedicated launchers of the first upgrade shall be used.

Summing up, AUG now has an EC system of eight beam lines with a nominal installed power of 8 MW at 140 GHz or 6.4 MW at 105 GHz. Due to power limitations on some gyrotrons of the first upgrade and including 13% losses in beam preparation and transmission, the maximum expected power in the plasma at 140 GHz is ≈6.5 MW. So far, 5.4 MW is regularly reached, limited mainly by arcing in the air-filled transmission lines. As described in [22] several hardening measures allowed us to regularly reach long pulses with the nominal power in one upgraded beam line such that operation above the 6 MW level seems feasible after upgrading the others later this year. In the context of this paper there is no space to discuss passive and active measures of machine protection against EC operation errors or excessive stray radiation. For AUG, these are described in [23, 24]. Some of the physics studies reported in section 3 made use of a replacement algorithm of the discharge control system (DCS) managing an abundance of operation-ready gyrotrons. A predefined waveform on the number of required gyrotrons is used by the DCS to request active gyrotrons according to a priority list. The DCS sends requests directly to the fast timing systems of all allocated gyrotrons, which have to be preset to listen to external control. The fast timing systems send availability signals to the DCS, which may indicate the encounter of a non-recoverable failure of a gyrotron during a pulse. In such an event, the DCS will replace that gyrotron by chosing from the still available gyrotrons according to the priority list. This is a relatively simple example of actuator management, which is actually developed further by the CODAC group of AUG [25].

3. ECRH/CD as a tool to test fusion-reactor physics

In the following, some EC applications on AUG are discussed, creating specific plasma states which allow us to answer open questions of reactor physics. We start this section by mentioning that many of the cases discussed below require a mix with neutral beam injection (NBI) heating

(on AUG up to 20 MW) and ion cyclotron resonance heating (ICRH). In AUG, ICRH is typically applied as H-minority heating, regularly with powers above 4 MW in the plasma.

Most of the H-mode studies available worldwide today were done using NBI dominantly, with energies below 130 keV limited by the neutralization efficiency of the accelerated H^+ ions. Confinement- and L/H threshold scalings are possibly biased by this heating method, which leads to dominant ion heating typically at low collisionalities, with many high performance plasmas being characterized by $T_i > T_e$. In ITER it cannot be expected that $T_i > T_e$ since most of the heating is applied to the electron channel (α-heating and 1 MeV NBI). It is therefore crucial to study the influence of T_e/T_i experimentally and theoretically to validate the codes used for the experimental planning in ITER. Additionally, in a reactor plasma one has to keep in mind the shifted balance between radial energy fluxes characterized by the time scale τ_E and the local heat exchange terms between electrons and ions characterized by the time scale $\nu_{ei,E}^{-1}$.[9] The dimensionless number $\tau_E \times \nu_{ei,E}$ is a coarse measure to compare the effect of equilibration fluxes (assuming self similar kinetic and heating profiles). As a consequence, the distribution of the plasma heating between the electron and the ion channel has far less of an effect on, for example, the ratio T_e/T_i in a reactor plasma (for which the ratio is close to unity), than in a plasma of similar collisionality in a smaller machine. This is at least the case during the burn phase of ITER, when H-mode will be reached and $\tau_E \nu_{ei,E}$ will be at maximum, but not necessarily for operation in L-mode with low plasma currents as it will occur at the beginning and end of all discharges and in particular in the commissioning phases of a new machine (ITER PFPO-1 in 2028) [16].

Another significant difference between the typical NBI-heated plasmas of today and future reactors is the ratio of torque (due to NBI) and the moment of inertia being much smaller for the future reactors such that a much smaller rotational shear is expected. This shear is known to reduce the strength of micro-turbulence (see the discussion in section 3.3). On AUG, wave-heating schemes offer momentum-free heating for comparison. (Another route has been chosen by DIII-D using balanced NBI, which comes with increased fast ion losses for those injected with a velocity component opposite the plasma current [26]. The corresponding effects need to be separated carefully.)

Apart from delivering highly localized pure electron heating with no torque, the EC has the potential to drive toroidal electric current. The direction can be changed, modifying the toroidal launcher angle (co-ECCD, ctr-ECCD). In this article we deliberately exclude the effect of very localized ECCD close to resonant surfaces, as used to influence macroscopic Magnetohydrodynamic (MHD)-modes, although at least the stabilization of (2,1)-NTMs is considered a major application of the EC in a reactor in order to stay away from disruptions. The remaining questions in that field

address matters of technical realizations, diagnostics and algorithms rather than matters of fundamental physics. Far less understood is the effect of non-standard current profiles on tokamak operation, i.e. deviating from the shape determined by the profiles of ohmic and bootstrap current combined with quasi-periodic redistribution due to the sawtooth instability inside the $q = 1$ surface. Non-standard current profiles are typically achieved by applying external current drive with NBCD, ECCD and also lower hybrid waves (LHCD) [27]. An ultimate goal is the fully non-inductive reactor operation based only on bootstrap current and (as little as possible) external current drive. Such a plasma state is dominated by a coupled non-linear interplay of locally reduced transport in the ion and/or electron channel, the corresponding bootstrap current, the dependence of the externally driven current profile on the kinetic profiles, the dependence of the local transport and the plasma stability (β-limit) on details of the q-profile (which is determined by the current profile), the α-particle heating which depends on the kinetic profiles, and the ohmic transformer itself which acts as a buffer for excessive or missing current drive; not to mention the effects of the plasma shape, such as, for example, triangularity. While it may be interesting from a control point of view to access this operational point exactly in present day devices, one should consider that there is no way to mimic a future reactor in a dimensionless way in today's devices, similar to the discussion about $\tau_E \times \nu_{ei,E}$ above. Low collisionality is a general prerequisite for an efficient external current drive. As a consequence, strong ECCD in small machines increases the ratios of T_e/T_i, and NBCD based on the acceleration of positive ions reduces this ratio. The profiles of driven currents are very different for both systems, and the ratio T_e/T_i can have a strong effect, especially on the ion transport [28]. This leads to a coupling of the external current drive and ion transport, which will be much weaker in a reactor. A similar mechanism may be driven via the effect of NBCD and ECCD on rotational shear, which also affects ion transport. The only reliable way to use present day experiments to predict reactor performance is to develop, challenge and optimize models for the underlying physics as close as possible to first principles. The topics discussed below should be regarded as incomplete examples.

## 3.1. Transport of energy and particles

As mentioned in the introduction, the first EC system of AUG has already been used to study energy and particle transport, focusing on heat-pulse propagation and variations in the density profile in L-mode. With more EC power these experiments could be extended to H-modes [28, 29]. The trapped gyro Landau fluid code TGLF [30, 31] was successfully used to model discharges with varying heating mix and thus significant variation in T_e/T_i and rotational shear [32, 33], indicating that energy and electron transport well inside the H-mode barrier is reasonably well understood on a first principle basis. More uncertain is the quantitative description/prediction of rotation and impurity profiles. Trends of the variation in the rotation profile with the heating mix and torque input were reproduced

---

[9] The collisionality $\nu_{ei,E}$ is smaller than the collisionality for the momentum exchange ν_{ei}, related to a 90° deflection of the electron velocity due to collisions with ions. The ratio is m_e/m_i making $\nu_{ei,E}$ isotope dependent.

correctly and were related to the dominant instabilities [34, 35]. The focus on ECRH studies with impurities was enforced by the W programme of AUG, which culminated in the first operation of a diverted high-power plasma with completely W-coated first wall surfaces. Empirically, it was found that ECRH was essential to prevent collapses due to central W accumulation, particularly for cases with low gas puff and low safety factor [36]. The plans to use W or its alloys as first wall material for ITER and future reactors motivated studies on W transport, not only on AUG but also on JET or other machines, which covered some high erosion surfaces with W. It turned out that the good localization of electron heating in the center together with a source-free penetration of the heating power across the plasma edge were key elements to prevent W accumulation with EC. The latter point was the essential difference to IC until new IC antennas were developed, minimizing oscillating electric fields at the antenna frames, which, by sheath rectification, lead to the acceleration of light impurities such as oxygen or nitrogen to energies sufficient to sputter W from the limiters [37]. Using the new IC antennas, it could be shown that electron heating by IC had similar effects on the peaking of the W profile as the EC [38]. Only for the cases with strong, highly localized central EC heating differences were observed, possibly due to effects of the localized power on MHD-modes, as described in [39]. A mainly theoretical paper on W transport in AUG and JET is [40]. With respect to ITER, it helps that the ratio of neoclassical to turbulent transport reduces strongly with machine size. Since the inward transport of W is dominantly a neoclassical effect, it is reduced significantly in ITER such that no W accumulation is expected [41]. EC would have been inadequate as a tool to increase central electron heating strongly since α- and NBI-heating are the dominant sources. Experimentally, on AUG ≈ 2 MW of central EC are sufficient in order to suppress W accumulation, thus the EC upgrade was not strictly necessary to extend the operational range with respect to q_{95} or minimum gas puff, but it allows a further variation of the heating profiles for those conditions. A general problem for W transport studies is to obtain a good resolution of the W profile by spectroscopy [42]. This is easier for lighter impurities which exhibit distinct excited states after charge exchange with fast deuterium ions from NBI. The charge exchange recombination spectroscopy diagnostic can be tuned to deliver profiles for such impurities. It turned out that boron is well suited for such studies as it can be introduced into the machine via boronisation, and its influx can be modulated by varying the ion cyclotron range of frequencies power. The technique is described in [43]. Such experiments with varying amounts of EC have been carried out and compared to theory [44].

3.2. H-mode access and of edge localized modes-free operation

These two topics are of crucial interest to ITER, which aims to access H-mode as early as possible to develop scenarios of H-mode operation without of edge localized modes (ELMs). As described above, these plasmas shall be run at a third of the full magnetic field and current, thus at rather low densities either in
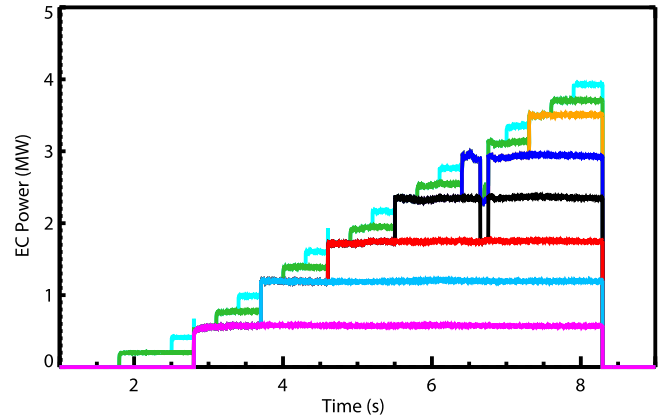

Figure 1. A power ramp running two gyrotrons with reduced cathode and body voltages at 200 kW (in plasma) and the other six at 600 kW (AUG #35970). Gyrotron on/off wave forms are set in the discharge program; power levels have to be preset by the EC operators.

hydrogen or helium and heated only by ECRH, which shall be the first of the three heating systems (NB, IC, EC) to be available. A first question relates to the minimum density, above which the scaling for the L/H transition [45] can be considered as valid in ITER. A model for this minimum density has been developed at AUG [46], relating the L/H transition to the heat flux in the ion channel. Such a model can of course only be developed if the heat flux in both channels can be varied significantly. Recent experiments with high-power EC strongly support this model: at very low densities (1×10^{19} m^{-3}) where coupling between electrons and ions is very low, L-modes can be heated with more than 5 MW without a sign of L/H transition, which exceeds the minimum power by more than a factor of three (required at the lowest density for which the scaling is valid, i.e. 4×10^{19} m^{-3}). The complete EC system of eight gyrotrons allows the running of finely-tuned power ramps to study threshold behavior (figure 1). Running two gyrotrons with reduced cathode- and body-voltages at 200 kW and the others at 600 kW, the system can be ramped in 20 steps or 0.2 MW up to 4 MW[10].

With ramps like this the dependence of the L/H threshold power on the ion mix has been studied for H/D and H/He mixtures. These studies were triggered by similar experiments at JET [48], in which it was found that small additions of He or D to hydrogen-plasmas did reduce the L/H power threshold significantly, which would be helpful for early H-mode access in hydrogen in the non-nuclear phase of ITER. On AUG, the threshold power also shows a non-linear dependence. However, in contrast to JET, small additions have essentially no effect, but changes occur in a small window of intermediate mixtures, as discussed at this conference in [49]. The EC power ramps were also used in combination with gas puff ramps to characterize H-mode

---

[10] This does not mean that all beams are absorbed exactly at the same value of ρ, which would require iterative tuning or online control of the launching angles [47]. For so-called 'central heating' at $B_t = 2.45$–2.55 T, a standard set of launching angles is used which results for the vast majority of AUG plasmas in heat deposition inside $\rho_{tor} < 0.2$, sufficient to prevent W accumulation.
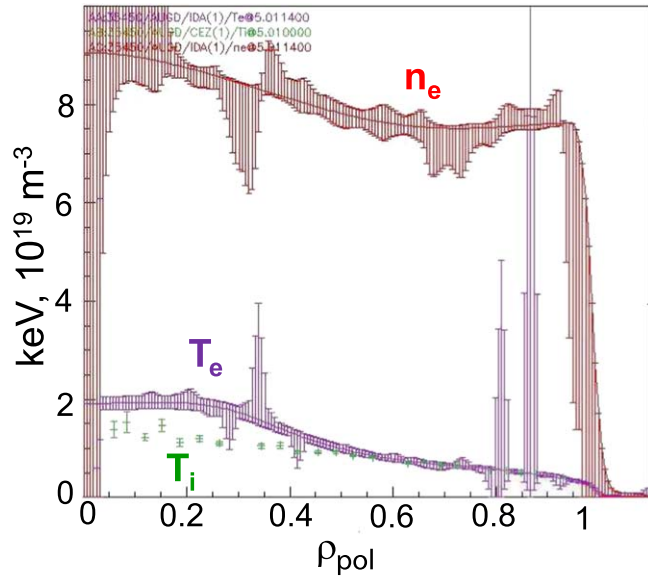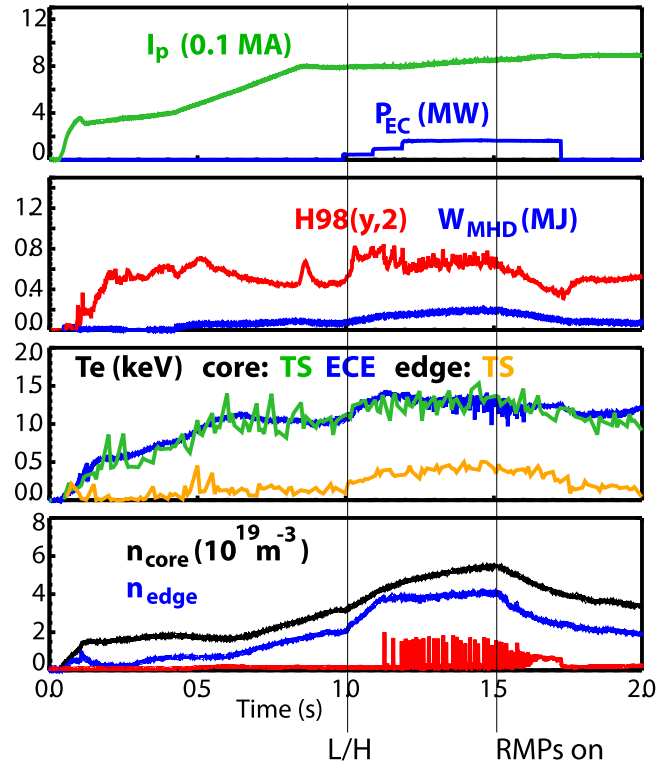
Figure 2. Kinetic profiles for AUG discharge 35450 at $t = 5$ s: $I_p = 0.8$ MA, $B_t = 2.5$ T, $P_{EC} = 1.6$ MW, $P_{OH} = 0.3$ MW, $\tau_E = 180$ ms, $n/n_{GW} = 0.85$.

Figure 3. X3 heating in AUG (# 35553) without NBI (on error). The phase of interest here ends at 1.5 s when RMP coils affect the H-mode pedestal, where the EC is dominantly absorbed. The reduction of pedestal pressure leads to incomplete absorption and the EC is switched off due to excessive stray radiation. $T_e(0)$ from electron cyclotron emission (ECE, blue) and Thomson scattering (TS) (green), $T_{e,ped}$ from TS (orange).

operation just above the L/H transition, where according to the H-mode confinement scalings [50] τ_E is largest as it decreases with increasing additional power. Not surprisingly the ITER operational point is close to this threshold. As a result of these scans, a new EC-only ELM-free H-mode regime with a stationary pedestal was found, seemingly stabilized by a density fluctuation in the pedestal region of several 10 kHz, resembling the enhanced D-α (EDA-)mode of Alcator C-Mod with its quasi coherent mode [51].

As figure 2 shows, for this purely electron heated H-mode, T_e and T_i are identical outside $\rho_{tor} > 0.4$, and in the center T_i is only 20% lower. The density reaches 85% of the Greenwald limit n_{GW}, as planned for ITER. Due to the high $\tau_E = 0.18$ s, which is about 1/20 that of ITER (Q = 10), and a collisionality about 20 times higher than in ITER the product $\tau_E \nu_{ei,E}$ is rather close for these discharges to the ITER Q = 10 scenario. In [52] TGLF has been used to model the ITER Q = 10 scenario, applying a fictive 40 MW of EC as only additional heating in order to check the effect of pure EC heating in ITER on T_e/T_i, yielding a similar $T_i(0) \approx 0.8 T_e(0)$. TGLF modeling of these new data is planned. For further discussion of this new ELM-free regime see [53].

At ITER, for the H-mode attempts in PFPO-1 with 1/3 B_t (1.8 T), it would be cost efficient to use the 170 GHz system under construction at the third harmonic, i.e. X3 heating starting after ohmic current ramp up [54]. As mentioned above, absorption, especially at low temperatures, is very poor, but increases quadratically with T_e. A kind of bootstrap process can be expected if the radial energy transport is small enough. Assuming or modeling this radial transport, the minimum power to be absorbed at the X3 location to trigger such a process can be calculated as a function of the initial temperature. An X3-heating scenario is regularly run on AUG to support the ELM-suppression experiments with coils generating resonant magnetic perturbations (RMPs) [55] with central electron heating at low

q_{95}, but in contrast to the ITER case the plasma is pre-heated with NBI. The results are well in line with the expectations from TORBEAM. Under these circumstances, single pass absorption is around 80% and exceeds 90% as the central electron temperature reaches 4 keV. Note that there is no need for modifications of the electron energy distribution by additional lower frequency EC heating at X2, as reported from TCV [56]. In the database, a case was found without NBI with close to 2 MW of EC, shown in figure 3. Under the specific conditions of AUG the X2 resonance is still in the plasma on the high-field side (HFS), and the power passing the X3 resonance is absorbed there. The X3 single pass absorption is ≈10% at the time EC is switched on. Subsequently the edge temperature rises by a factor of four also, because the first EC beam immediately triggers the L/H transition. So this is not yet the real ITER case, but a safe test bed for the initial study of the bootstrap process with up to 5.5 MW. Systematic studies and validation of the model used for ITER are planned in the frame of the ITER-IOS group. In ITER, such a safe operation using X3 with an X2 dump on the HFS would require $B_t >= 2.1T$. That choice would also shift the X3 power-deposition more on the axis where T_e is highest, and would reduce the volume of the flux surface where the power is deposited, i.e. it would significantly increase the power density as a function of ρ, but of course comes with a potential increase in the L/H threshold by 17%. It may still be an interesting option for the initial verification of models.

3.3. Non-inductive operation with co-ECCD

In AUG, H-mode operation with low gas puff had to be re-established over several years after all the plasma facing components were covered with W. Aside from applying sufficient EC, this optimization included the development of plasma shapes with high wall clearance, modification of the gas puff to compensate for the difference in fuel retention of graphite and W and optimization of NB and EC time traces in order to pass between decoupling of electrons and ions (too much EC) and W accumulation [57]. Having mastered these issues, the collisionality was low enough to use the EC as a versatile tool for current drive. Using half of the actual EC power, close to non-inductive H-modes were obtained at $q_{95} = 5.3$, which is already close to the values foreseen for ITER non-inductive operation ($q_{95} = 5.0$) or DEMO ($q_{95} = 4.5$). Performance was limited by ideal modes at $\beta_N \approx 2.8$ [58, 59]. After redirecting one gyrotron closer to the axis in order to become less dependent on wall conditions and W accumulation the beta limit increased to 3.0, indicating a high sensitivity to details of the current profile. A further increase to 3.2 was achieved [60], minimizing dynamic error fields by an optimized setting of the RMP coils using the CAFE code [61]. A steepening of the ion temperature inside $\rho_{tor} \approx 0.5$ at high β was essential for high bootstrap current. Initial modeling with TGLF could not reproduce this steepening, triggering analysis using the gyrokinetic code GENE. With GENE it was found that the effect of β of the fast ions, and to a similar degree β of the thermal plasma, contributed significantly to the steepening of ∇T_i [62]. Contrary to this, colleagues from EAST re-analyzing AUG data found good agreement with TGLF [63]. The contradiction was resolved and the modification to the effect of the rule handling the stabilizing effect of ExB shear [64] could be identified as the dominant effect (changing from α_quench to α_e) [65]. This is in line with older results which identified the ExB shear as a major ingredient to steepen ∇T_i [5], also backed by GS2 calculations and with ctr-NBI experiments at DIII-D [66] compared to GLF23. In contrast, further GENE analysis for the non-inductive AUG-discharges discussed here did not show a significant reaction of ∇T_i on the variation of ExB shear. To resolve this experimentally, NB heating in these discharges was partially replaced by IC, which in AUG has a heating mix close to that of NB, avoiding the negative effects of very strong EC heating on ion transport as discussed above. As shown in figure 4, essentially all central NB heating was replaced by IC, keeping on the two off-axis beams, which drive 40% of the total current. This strong reduction of the central torque reduces the ExB shear by 60% in the radial range of the steep ∇T_i. The figure also shows that $T_i(\rho = 0) - T_i(0.3)$ hardly changes for the two indicated intervals with constant β. This seems to support the GENE analysis. Still, the IC and central NB have different deposition profiles, thus the absolute values of the heat fluxes changed in the plasma center. A detailed analysis of the new data with TGLF and GENE is necessary to draw conclusions. More details will be presented in [65].

3.4. q-profile tailoring with ctr-ECCD

A major goal of the AUG program to be tackled by doubling the installed EC power from 4 to 8 MW, is the study of stationary H-modes with elevated q-profiles with variable degrees of inversion towards the axis. For the collisionalities and electron temperatures in AUG, ECCD in the outer half of the plasma radius is rather inefficient. Such a type of co-current drive would be necessary to elevate and invert the q-profile, since it basically means shifting the current from inside of the envisaged $\rho(q_{\min})$ to larger radii. The situation may be facilitated by the formation of internal transport barriers (ITBs), which lead to a localized off-axis bootstrap current and low bootstrap current in the plasma center. On the other hand, such ITBs often also reduce impurity transport leading to central accumulation of heavy ions. The low central current density reduces the confinement of fast ions in the plasma center. Additionally, strong pressure gradients and wide or even hollow current profiles are prone to MHD instabilities. The connection between q-profile shape, in particular q-profile inversion and ion transport, which is often used to model the self-sustainment of ITBs by the bootstrap current they generate, is empirically by far not as well documented as it is for electron ITBs at very low density with central ctr-ECCD [67]. The physics studies on AUG shall focus first on the relation between the q-profiles, ion transport and MHD-stability, which has to be treated correctly in any model addressing non-inductive reactor operation. With ECCD this can be done most efficiently by applying broad ctr-ECCD profiles in the inner part of the plasma, leading to an increased ohmic current across the whole radius. This ohmic current is overcompensated by ctr-ECCD in the inner part. In other words we use a large part of the ctr-ECCD to drive the ohmic current effectively off-axis, and use only a small part of the ctr-ECCD for the central inversion of the q-profile. This is definitely not the way such profiles shall be generated in a non-inductively running reactor, but a way forward to generate such profiles over several current diffusion times in AUG such that terms related to time derivatives shall ring down to reduce the unknowns entering the interpretation. Still, this concept comes with some potential incompatibilities which require optimization: since strong central ECCD comes with strong central electron heating it will lead to the formation of electron ITBs if the density and/or the ion heating are too low. In AUG, such behavior was found for 600 kA, 2.5 T discharges, for which inverted q-profiles with $q_{\min} \approx 3$ were achieved with $T_e \gg T_i$. A higher plasma current increases τ_E and the density and thus strongly the coupling between electrons and ions. The drawbacks are less current drive efficiency (and higher total current) and smaller achievable $\beta_{pol} \propto \beta_N B_t / I_p$ for fixed $\beta_{N,\max}$ and B_t. This leads to less bootstrap current, and would reduce any beneficial effects of high β_{pol} on ion confinement. Thus, the current has to be minimized such that operation without electron ITBs is possible close to the β-limit with full ctr-ECCD. The corresponding value of q_{95} should be close to the values foreseen for ITER and DEMO, i.e. 4.5–5.0. Experiments have so far been extended to 800 kA ($q_{95} = 5.0$)
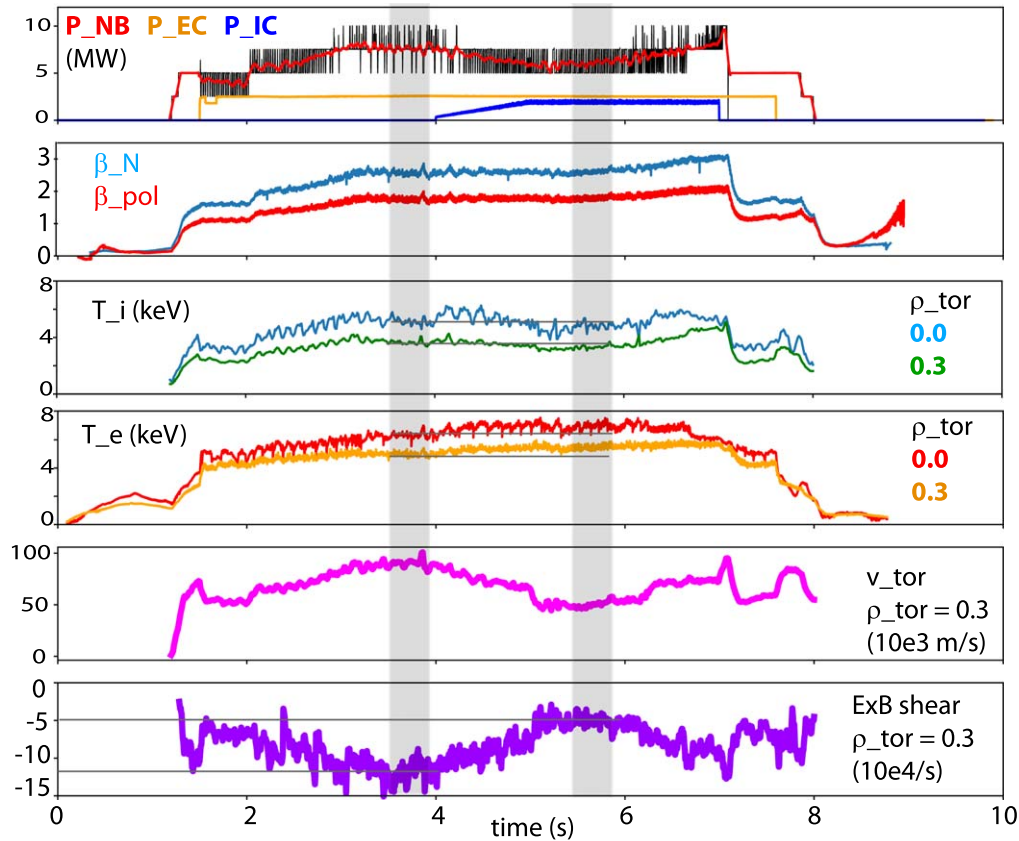
Figure 4. AUG discharge #35938, over 90% non-inductively driven H-mode similar to [58]. The NB is running under β-control. The frame at the top shows the heating powers. The IC is feed-forward controlled, and as it sets in at 4s, NB is reduced to keep β constant until towards the end β is ramped up. The lower two traces show the effect on toroidal rotation and ExB shear at $\rho_{tor} = 0.3$. The two frames in the middle show time traces of T_e and T_i at $\rho_{tor} = 0$ and $= 0.3$. The grey vertical bars indicate the time intervals to be compared, taking into account overshoots of the β-control. During these phases β (2nd from top) is close to equal, but the shear is significantly different. The horizontal lines are meant to facilitate comparison of the data.

and 1 MA ($q_{95} = 4.0$). For 800 kA, difficulties have been encountered with strong (2,1) MHD, violently appearing during q-profile evolution. For this plasma current, the q-profile shows a rather flat shear close to $q = 2$. The working hypothesis is that the (2,1) mode is triggered as the flat shear region crosses the $q = 2$ surface during current profile evolution. As a consequence, the 1 MA scenario was developed, applying an external current drive after an ohmic q-profile at full current was formed. This allows us to approach the equilibrated q-profile, which has $q_{min} < 2$ from the low q_{min} side.. During this development it was important to have a reliable diagnostic for the current profile, since the actual current profile is a small difference of large numbers due to the use of ctr-ECCD. In [68] this is described in detail. Here, we note that internal measurement polarimetry [69] and imaging motional Stark effect [70] are used, and the result is well in line with NBCD calculations from RABBIT [71], ECCD calculations from TORBEAM and the neoclassical current diffusion. These discharges are typically free of large scale MHD instabilities, except for the ELMs, the violent (2,1) modes mentioned above and the ideal modes which set the limit for β_N. Figure 5 shows the status achieved so far for the 1 MA case. As the time traces indicate, T_e is in the center always higher than T_i. The T_e profile is strongly peaked

towards the center and hardly changes as the q-profile evolves (profile plots A, B on the right). T_i clearly changes; it steepens and approaches T_e, except for the very center. The discharge at this high $\beta_N \approx 2.7$ has an H98(y,2) factor of 1.25, which is similar to that of improved H-modes stabilized by (3,2) NTMs with the same current, field and β_N not using any ECRH [72]. Towards the end of the discharge the β request is increased leading to MHD stabilities. Options for further improvement are the increase in triangularity (and thus density), or to widen the ECCD profile in the center or to reduce the plasma current to test whether the increase in ion heating and β_{pol} has a steepening effect on the ion temperature. For the discharge shown in figure 5, the ECCD profile and the driven current profile, as well as an error discussion, can be found in [68]. Comparisons with TGLF are planned, after the discrepancies with TGLF and GENE are analysed, as discussed in section 3.3.

4. Summary and conclusions

The EC system of AUG has become a central element of the tokamak operation, essential for studying a wide spectrum of physics questions, which could be addressed here only in examples not in completeness. The necessity to understand
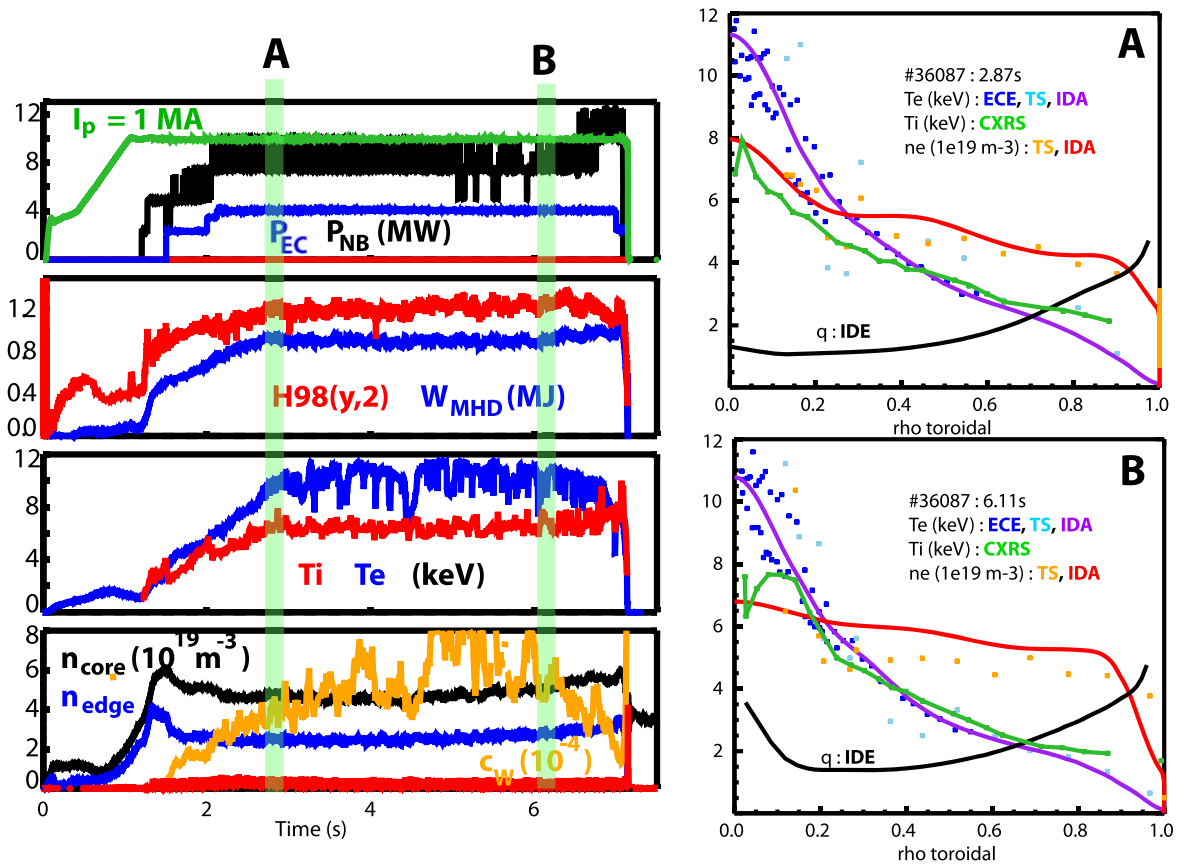
Figure 5. AUG # 36087: ctr-ECCD combined with mainly off-axis NBCD in order to elevate and broaden the q-profile. Frames A, B show profiles at the beginning and the end of the constant β phase, as marked on the left. The profiles marked 'IDA' result from integrated data analysis [73], fitting a n_e-profile to lithium beam and interferometry data, which is then used to fit a T_e-profile to the ECE data. The NB is operating under β-control, as in figure 4; a beta ramp starts at 6s, as seen on the W_{mhd}-trace.

and model the underlying physics has been stressed as the key tool for extrapolation of the plasma behavior in existing devices to reactors. With respect to the EC, caution has to be taken with all effects involving changes in the T_e-profile, in the ratio T_e/T_i or in rotation. The corresponding effects will be much smaller in a reactor dominantly heated by α-particles with marginal torque input and large $\tau_E \nu_{ei,E}$ than in today's NB-heated low collisionality plasmas. This should also be considered for control studies driven by the urgent needs of ITER to suppress instabilities leading to disruptions, confinement loss or fast particle losses. As an example, EC has been proposed for control of Alfvén eigenmodes [74]. A detailed analysis has meanwhile shown that the initially observed effects on these modes were due to changes in T_e and are thus not transferable to a reactor [75]. The same is true for W accumulation, as discussed in section 3.1. Any actuator will only be effective if it has the potential to significantly change the quantity to be controlled. For the EC in the burning ITER plasma, besides its general heating potential, these specific potentials are the dominating very narrow local current drive capability of the upper launchers to be used for NTM control, and, especially for the non-inductive scenario, the variability of the ECCD capability of the equatorial launcher which may be used to fine-tune the q-profile, as discussed above for AUG.

Acknowledgments

ORCID iDs

J Stober ⓘ https://orcid.org/0000-0002-5150-9224
A Bañón Navarro ⓘ https://orcid.org/0000-0003-0487-6395
T Görler ⓘ https://orcid.org/0000-0002-0851-6699
V Igochine ⓘ https://orcid.org/0000-0003-2045-2998
R McDermott ⓘ https://orcid.org/0000-0002-8958-8714
Th Pütterich ⓘ https://orcid.org/0000-0002-8487-4973

References

[1] Prater R 2004 *Phys. Plasmas* **11** 2349–76
[2] Poli E 2018 *Computer Phys. Comm.* **225** 36–46
[3] Leuterer F *et al* 2009 *Fusion Sci. Tech.* **55** 31–44

[4] Ryter F, Angioni C, Peeters A G, Leuterer F, Fahrbach H U, Suttrop W and (ASDEX Upgrade Team) 2005 *Phys. Rev. Lett.* **95** 085001

[5] Manini A, Angioni C, Peeters A G, Ryter F, Jacchia A, Maggi C F, Suttrop W and (ASDEX Upgrade Team) 2006 *Nucl. Fusion* **46** 1047–53

[6] Angioni C, Peeters A G, Ryter F, Jenko F, Conway G D, Dannert T, Fahrbach H U, Reich M, Suttrop W and (ASDEX Upgrade Team) 2005 *Phys. Plasmas* **12** 040701

[7] Gantenbein G, Zohm H, Giruzzi G, Günter S, Leuterer F, Maraschek M, Meskat J, Yu Q and (ASDEX Upgrade Team, ECRH Group) 2000 *Phys. Rev. Lett.* **85** 1242–5

[8] Maraschek M, Gantenbein G, Yu Q, Zohm H, Günter S, Leuterer F, Manini A and (ECRH Group, ASDEX Upgrade Team) 2007 *Phys. Rev. Lett.* **98** 025005

[9] Mück A, Goodman T P, Maraschek M, Pereverzev G, Ryter F, Zohm H and (ASDEX Upgrade Team) 2005 *Plasma Phys. Controlled Fusion* **47** 1633–55

[10] Manini A, Maraschek M, Cirant S, Gantenbein G, Leuterer F, Zohm H and (ASDEX Upgrade Team) 2006 Optimisation of MHD stability using ECCD in ASDEX Upgrade *Proc. of. XIV Joint Workshop on Electron Cyclotron Emission and Electron Cyclotron Heating (EC-14) (Santorini)*

[11] Igochine V, Chapman I T, Bobkov V, Günter S, Maraschek M, Moseev D, Pereversev G, Reich M, Stober J and (ASDEX Upgrade Team) 2011 *Plasma Phys. Controlled Fusion* **53** 022002

[12] Leuterer F *et al* 2003 *Fusion Eng. Design* **66-68** 537–42

[13] Wagner D *et al* 2008 *Nucl. Fusion* **48** 054006

[14] Wagner D (ASDEX Upgrade Team) *et al* 2014 *International Conference on Infrared, Millimeter, and Terahertz Waves (IRMMW-THz), 2014 XXXIX* 1–2

[15] Ikeda R, Oda Y, Kobayashi T, Kajiwara K, Terakado M, Takahashi K, Moriyama S and Sakamoto K 2017 *J. Infrared Millim. Terahertz Waves* **38** 531–7

[16] ITER Organization 2018 *ITER Research Plan Within the Staged Approach (level III-Provisional Version) Tech. Rep. ITR-18-003* Appendix G URL (https://iter.org/doc/www/content/com/Lists/ITERTechnicalReports/Attachments/9/ITER-Research-Plan_final_ITR_FINAL-Cover_High-Res.pdf)

[17] Reich M *et al* (ASDEX Upgrade team) 2014 Real-time control of NTMs using ECCD at ASDEX Upgrade *Fusion Energy, XXV. Int. Conf., St. Petersburg (IAEA)* PPC/P1–26

[18] Höhnle H *et al* (ASDEX Upgrade Team) 2011 *Nucl. Fusion* **51** 083013

[19] Wagner D *et al* (ADSEX Upgrade Team) 2016 Extension of the multi-frequency ECRH system at ASDEX upgrade *2016 XLI International Conference on Infrared, Millimeter, and Terahertz waves (IRMMW-THz)* 1–2

[20] Schubert M *et al* (ASDEX Upgrade Team) 2017 *EPJ Web Conf.* **157** 03047

[21] Schubert M *et al* (ASDEX Upgrade Team) 2019 *EPJ Web Conf.* **203** 2009

[22] Wagner D *et al* (ADSEX Upgrade Team) 2019 Completion of the 8 MW Multi-frequency ECRH System at ASDEX upgrade *2019 XLIV International Conference on Infrared, Millimeter, and Terahertz Waves (IRMMW-THz)* 1–2

[23] Schubert M, Honecker F, Monaco F, Schmid-Lorch D, Schütz H, Stober J, Wagner D and (ASDEX Upgrade Team) 2012 *EPJ Web Conf.* **32** 02013

[24] Schubert M *et al* (ASDEX Upgrade Team) 2015 *EPJ Web Conf.* **87** 02010

[25] Kudlacek O, Treutterer W, Janky F, Sieglin B and Maraschek M 2019 *Fusion Eng. Des.* **146** 1145–8

[26] Solomon W M *et al* 2013 *Nucl. Fusion* **53** 093033

[27] Gormezano C, Challis C D, Joffrin E, Litaudon X and Sips A C C 2008 *Fusion Sci. Tech.* **53** 958–88

[28] Ryter F *et al* 2019 *Nucl. Fusion* **59** 096052

[29] Angioni C, McDermott R, Fable E, Fischer R, Pütterich T, Ryter F, Tardini G and (ASDEX Upgrade Team) 2011 *Nucl. Fusion* **51** 023006

[30] Staebler G M, Kinsey J E and Waltz R E 2005 *Phys. Plasmas* **12** 102508

[31] Staebler G M, Candy J, Howard N T and Holland C 2016 *Phys. Plasmas* **23** 062518

[32] Sommer F *et al* (ASDEX Upgrade Team) 2015 *Nucl. Fusion* **55** 033006

[33] Fable E *et al* (ASDEX Upgrade Team) 2019 *Nucl. Fusion* **52** 076042

[34] Angioni C *et al* (ASDEX Upgrade Team) 2011 *Phys. Rev. Lett.* **107** 215003

[35] McDermott R, Angioni C, Conway G, Dux R, Fable E, Fischer R, Pütterich T, Ryter F, Viezzer E and (ASDEX Upgrade Team) 2014 *Nucl. Fusion* **54** 043009

[36] Gruber O *et al* (ASDEX Upgrde Team) 2009 *Nucl. Fusion* **49** 115014

[37] Bobkov V *et al* (ASDEX Upgrade Team, EUROfusion MST1 Team) 2017 *Plasma Phys. Controlled Fusion* **59** 014022

[38] Angioni C, Sertoli M, Bilato R, Bobkov V, Loarte A, Ochoukov R, Odstrcil T, Pütterich T, Stober J and (ASDEX Upgrade Team) 2017 *Nucl. Fusion* **57** 056015

[39] Sertoli M, Angioni C, Odstrcil T and (ASDEX Upgrade Team, EUROFusion MST1 Team) 2017 *Phys. Plasmas* **24** 112503

[40] Angioni C, Bilato R, Casson F, Fable E, Mantica P, Odstrcil T, Valisa M and (ASDEX Upgrade Team, JET Contributors) 2017 *Nucl. Fusion* **57** 022009

[41] Loarte A *et al* 2016 *Evaluation of Tungsten Transport and Concentration Control in ITER Scenarios 26th IAEA Fusion Energy Conf. (Kyoto)*

[42] Pütterich T, Neu R, Dux R, Whiteford A, O'Mullane M, Summers H and (the ASDEX Upgrade Team) 2010 *Nucl. Fusion* **50** 025012

[43] Bruhn C *et al* (ASDEX Upgrade Team) 2018 *Plasma Phys. Controlled Fusion* **60** 085011 corrigendum in preparation (http://stacks.iop.org/0741-3335/60/i=8/a=085011)

[44] McDermott R M, Manas P, Angioni C *et al* 2019 *Validation of Low-Z Impurity Transport Theory Using Charge Exchange Recombination Spectroscopy at ASDEX Upgrade 46th EPS Conference on Plasma Physics, Milano, invited talk I2.105*

[45] Martin Y R and Takizuka T 2008 *Journal of Physics: Conference Series* 123 012033

[46] Ryter F, Orte L B, Kurzan B, McDermott R, Tardini G, Viezzer E, Bernert M, Fischer R and (ASDEX Upgrade Team) 2014 *Nucl. Fusion* **54** 083003

[47] Reich M, Bilato R, Mszanowski U, Poli E, Rapson C, Stober J, Volpe F and Zille R 2015 *Fusion Eng. Des.* **100** 73–8

[48] Hillesheim J C *et al* 2018 *Implications of JET-ILW L-H transition studies for ITER XXVII IAEA Fusion Energy Conf.*

[49] Plank U, Pütterich T, Angioni C, Cavedon M, Kappatou A, McDermott R M, Schneider P A and (ASDEX Upgrade Team) 2019 H-mode power threshold studies at ASDEX Upgrade in mixed ion species plasmas *Europhysics Conference Abstracts (Proc. of the XLVI EPS Conference on Controlled Fusion and Plasma Physics) (Milano)* O2.111

[50] ITER Physics Basis 1999 *Nucl. Fusion* **39** 2204

[51] Greenwald M *et al* 2000 *Plasma Phys. Controlled Fusion* **42** A263–9

[52] Stober J *et al* (ASDEX Upgrade Team) 2015 *EPJ Web Conf.* **87** 02004

[53] Gil L *et al* (ASDEX Upgrade Team, EUROfusion MST1 Team) 2019 Stationary ELM-free H-mode in ASDEX Upgrade *Europhysics Conference Abstracts (Proc. of the*

XLVI EPS Conference on Controlled Fusion and Plasma Physics) (Milano) O2.110

[54] Micheletti D, Farina D and Figini L 2019 *EPJ Web Conf.* **203** 2009

[55] Suttrop W *et al* (ASDEX Upgrade Team, MST1 Team) 2018 *Nucl. Fusion* **58** 096031

[56] Alberti S *et al* 2002 *Nucl. Fusion* **42** 42–5

[57] Stober J *et al* 2016 *Advanced Tokamak Experiments in Full-W ASDEX Upgrade 26th IAEA Fusion Energy Conf. (Kyoto)*

[58] Bock A *et al* (ASDEX Upgrade Team) 2017 *Nucl. Fusion* **57** 126041

[59] Bock A *et al* (ASDEX Upgrade Team) 2018 *Phys. Plasmas* **25** 056115

[60] Voltolina D, Bettini P, Igochine V, Marrelli L, Pigatto L, Piron L, Zammuto I and (ASDEX Upgrade Team, MST1 Team) 2019 Vacuum estimation of error field correction on ASDEX Upgrade *Europhysics Conference Abstracts (Proc. of the XLVI EPS Conference on Controlled Fusion and Plasma Physics) (Milano)* P4.1099

[61] Bettini P, Finotti C, Grando L, Marchiori G and Specogna R 2017 *Fusion Eng. Des.* **123** 518–21

[62] Doerk H, Bock A, Siena A D, Fable E, Görler T, Jenko F, Stober J and (ASDEX Upgrade Team) 2018 *Nucl. Fusion* **58** 016044

[63] Jian X, Chan V S, Chen J, Bock A, Zohm H, Fable E, Reisner M, Guo W and Zhuang G 2019 *Nucl. Fusion* **59** 106038

[64] Staebler G, Candy J, Waltz R, Kinsey J and Solomon W 2013 *Nucl. Fusion* **53** 113017

[65] Reisner M, Stober J, Fable E, Bock A, Rittich D, Navarro A B, Sienna A D and (ASDEXUpgrade Team) 2019 to be submitted to Nuclear Fusion

[66] Politzer P *et al* 2008 *Nucl. Fusion* **48** 075001

[67] Bottino A, Sauter O, Camenen Y and Fable E 2006 *Plasma Phys. Controlled Fusion* **48** 215–33

[68] Fischer R *et al* (ASDEX Upgrade Team) 2019 Current profile tailoring with the upgraded ECRH system at ASDEX Upgrade *Europhysics Conference Abstracts (Proc. of the XLVI EPS Conference on Controlled Fusion and Plasma Physics) (Milano)* P1.1100

[69] Mlynek A, Casali L, Ford O, Eixenberger H and (ASDEX Upgrade Team) 2014 *Rev. Sci. Instrum.* **85** 11D408

[70] Burckhart A 2015 Design of the new imaging motional stark effect diagnostic at ASDEX Upgrade *Europhysics Conference Abstracts (CD-ROM, Proc. of the XLII EPS Conference on Plasma Physics, Lisbon, Portugal, 2015) (ECA vol 39E)* ed R Bingham *et al* (Geneva: European Physical Society) P1.143

[71] Weiland M, Bilato R, Dux R, Geiger B, Lebschy A, Felici F, Fischer R, Rittich D, van Zeeland M and (ASDEX Upgrade Team, Eurofusion MST1 Team) 2018 *Nucl. Fusion* **58** 082032

[72] Stober J *et al* (ASDEX Upgrade Team) 2007 *Nucl. Fusion* **47** 728–37

[73] Fischer R, Fuchs C J, Kurzan B, Suttrop W, Wolfrum E and (ASDEX Upgrade Team) 2010 *Fusion Sci. Technol.* **58** 675–84

[74] Zeeland M V *et al* 2016 *Nucl. Fusion* **56** 112007

[75] Sharapov S E *et al* 2017 *Plasma Phys. Controlled Fusion* **60** 014026